

Supplementary Appendix for

**Gram-negative trimeric porins have specific LPS binding sites that are essential for porin biogenesis.**

Wanatchaporn Arunmanee<sup>1</sup>†, Monisha Pathania<sup>1</sup>†, Alexandra S. Solovyova<sup>1</sup>, Anton P. Le Brun<sup>2</sup>, Helen Ridley<sup>1</sup>, Arnaud Baslé<sup>1</sup>, Bert van den Berg<sup>1\*</sup> and Jeremy H. Lakey<sup>1\*</sup>

<sup>1</sup>Institute for Cell and Molecular Biosciences, Newcastle University, Framlington Place, Newcastle upon Tyne, NE2 4HH, United Kingdom.

<sup>2</sup>National Deuteration Facility, Bragg Institute, Australian Nuclear Science and Technology Organisation, Locked Bag 2001, Kirrawee DC, NSW 2232, Australia.

†These two authors contributed equally to the paper.

\*Corresponding authors

**Table S1** (A) Data collection and refinement statistics for OmpE36

---

**Data collection**

Beamline	DLS i02
Wavelength	0.9796
Space group	P 2 <sub>1</sub>
Cell dimensions (a,b,c)	109.75 123.26 116.01
( $\alpha,\beta,\gamma$ )	90.00 91.01 90.00
Molecules/AU	6
Solvent content	65
Resolution (Å)	48.92-1.45
Completeness	99.6 (100)
Redundancy	3.7 (3.7)
Rmerge (%)	8.4 (78)
Rpim (%)	4.9 (46)
CC (1/2)	0.98 (0.62)

**Refinement**

Resolution (Å)	48.92-1.45
Reflections (n)	529555
R <sub>work</sub> /R <sub>free</sub> (%) <sup>*</sup>	15.2/17.8
Atoms (n)	
Protein/solvent	16245/1910
ligand/detergent	1239/231
B factors (Å <sup>2</sup> )	
Protein/solvent	17/30
ligand/detergent	37/42
Rmsd	
bond lengths (Å)	0.0095
bond angles (°)	1.5091
Ramachandran plot (%)	
Most favoured/disallowed	95.5/0.6
Molprobit clashscore	1.37

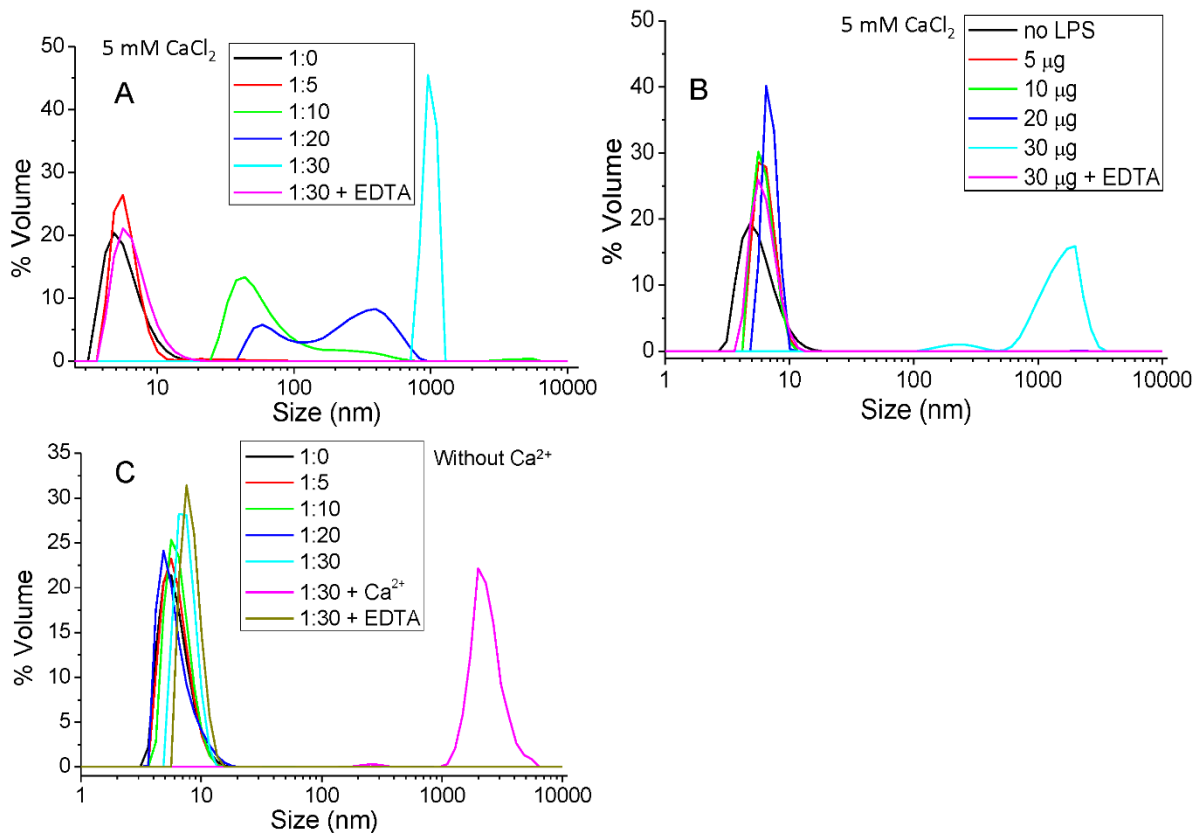
---

Values in parentheses refer to the highest resolution shell

\*R<sub>free</sub> was computed as for R<sub>work</sub> using a test set (5%) of randomly selected reflections that were omitted from the refinement

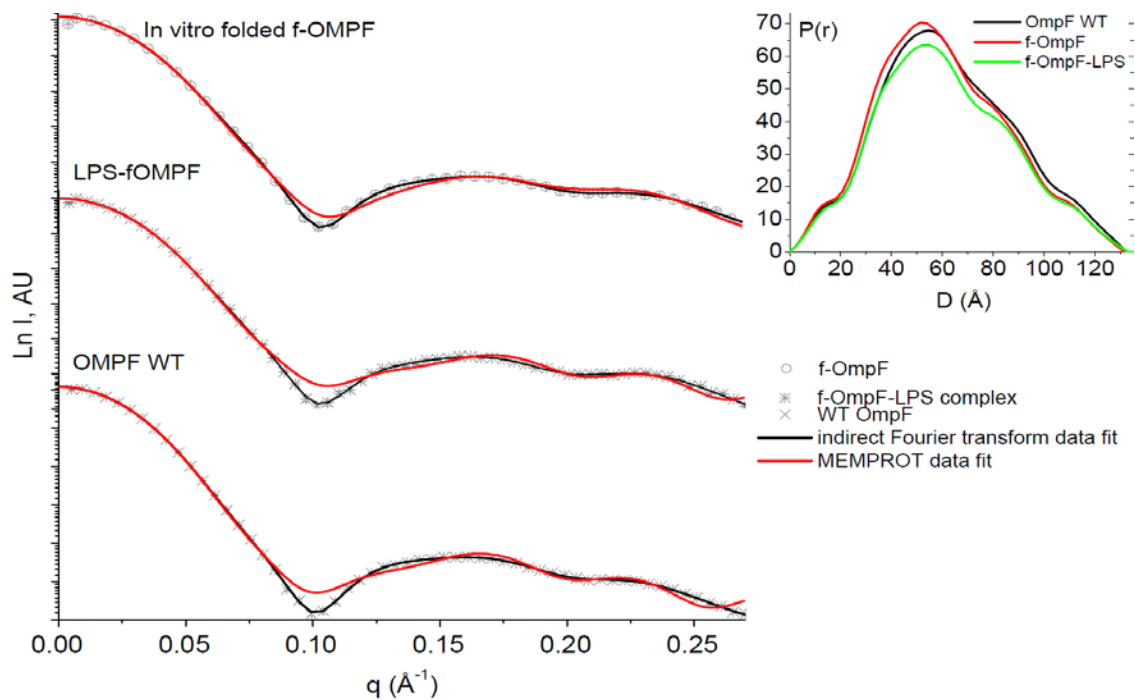
**Table S1 (B)** Interaction distances (in Å) measured for the OmpE36-LPS complex.

Residue of E36-C chain	LPS atom (moiety)	H-bond distance (2.3-3.6 Å)	Residue/LPS molecule	Metal ion	Ionic interaction distance (Å)
174 Asp, OH-	2 PA1, O4 (LPS-A)	2.63	250, Asn, O-	Calcium	2.36
174 Asp, OH-	3 GCS, N2 (LPS-A)	2.82	239, Asn, O-	Calcium	2.49
149 Tyr, OH-	7 FTT, O3 (LPS-A)	2.69	210, Asn, O-	Calcium	2.35
213 Arg, NH <sub>2</sub> -	11 MYR, O1 (LPS-A)	3.56	5, KDO, O7- (LPSB)	Calcium	2.59
213 Arg, NH <sub>2</sub> -	9 FTT, O2 (LPS-A)	3.6	5, KDO, O1- (LPSB)	Calcium	2.46
213 Arg, NH <sub>2</sub> -	6 PO <sub>4</sub> , O3 (LPS-A)	2.78	5, KDO, O5- (LPSB)	Calcium	2.45
198 Lys, NH <sub>2</sub> -	4 KDO, O1 (LPS-A)	2.84	5, KDO, O6- (LPSB)	Calcium	2.59
198 Lys, NH <sub>2</sub> -	3 GCS, O4 (LPS-A)	3.6			
198 Lys, NH <sub>2</sub> -	6 PO <sub>4</sub> , O1 (LPS-A)	2.8			
160 Asp, OH-	5 KDO, O5 (LPS-A)	2.52			
199 Arg, O-	5 KDO, O8 (LPS-A)	2.86	<b>28 hydrogen bonds between LPS (A or B) and OmpE36</b>		
159 Glu, O-	5 KDO, O4 (LPS-A)	2.8			
152 Lys, NH <sub>2</sub>	5 KDO, O1 (LPS-A)	2.91	<b>1 hydrogen bond between LPS A and LPS B</b>		
152 Lys, NH <sub>2</sub>	5 KDO, O6 (LPS-A)	3.2			
152 Lys, NH <sub>2</sub>	5 KDO, O5 (LPS-A)	2.81	<b>7 ionic interactions between calcium and LPS/OmpE36</b>		
201 Ser, NH-	5 KDO, O7 (LPS-A)	2.99			
<b>11 MYR, O1 (LPSA)</b>	<b>7 FTT, O3 (LPS-B)</b>	<b>3.09</b>			
213, Arg, NH-	7 FTT, O3 (LPS-B)	3.58	<b>Abbreviations</b>		
196, Ser, OG	7 FTT, O3(LPS-B)	2.9	2-amino-2deoxy-β-D-glucopyranose	GCS	
215, Glu, OH-	9 FTT, O2 (LPS-B)	3.23	2-amino-2deoxy-α-D-glucopyranose	PA1	
215, Glu, OH-	2 PA1, O4 (LPS-B)	2.41	3-deoxy-alpha-D-manno-oct-2-ulosonic acid	Kdo	
250, Asn, OH-	5 KDO, O5 (LPS-B)	3.11	3-hydroxytetradecanoic acid	FTT	
217, Tyr, OH-	9 FTT, O2 (LPS-B)	3.54	Dodecanoic acid	DA0	
239, Asn, NH-	5 KDO, O1A (LPS-B)	2.79	Tetradecanoic acid	Myr	
210, Asn, OH-	5 KDO, O5 (LPS-B)	2.94	L-glycero-alpha-D-manno-heptopyranose	GMH	
215, Glu, OH-	3 GCS, N2 (LPS-B)	3.14			
236, Gln, NH-	12 DAO, O1 (LPS-B)	3.31			
238, Tyr, OH-	6 PO <sub>4</sub> , O3 (LPS-B)	2.64			
238, Tyr, OH-	3 GCS, O4 (LPS-B)	3.58			
251, Lys, NH-	6 PO <sub>4</sub> , O3 (LPS-B)	3.43			



**Figure S1** Dynamic light scattering measurements of the effect of LPS-OmpF ratio and divalent cations on the formation of OmpF-LPS aggregates. (A) Size distribution of OmpF-Ra-LPS complexes studied by dynamic light scattering in 5 mM CaCl<sub>2</sub>, 1% SDS. (B) Increasing concentrations of Ra-LPS without OmpF in 5 mM CaCl<sub>2</sub>, 1% SDS. The signal in the zero LPS sample is from SDS micelles. In each case 10 mM EDTA was added to the 1:30 ratio sample which removed all calcium ions and returned the complex size to a similar value before calcium addition. (C) OmpF-Ra-LPS complexes in 1% SDS without added calcium except 1:30 when 5 mM CaCl<sub>2</sub> was added. This was followed by 10 mM EDTA to remove free Ca<sup>2+</sup>.

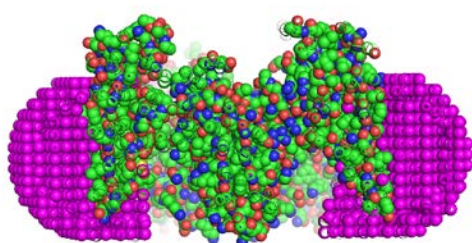
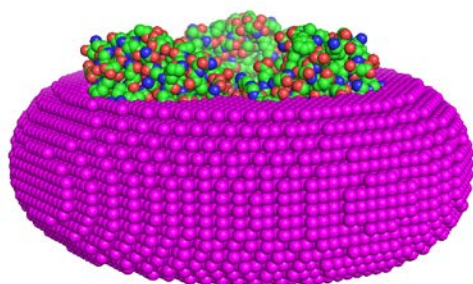
## S2:A



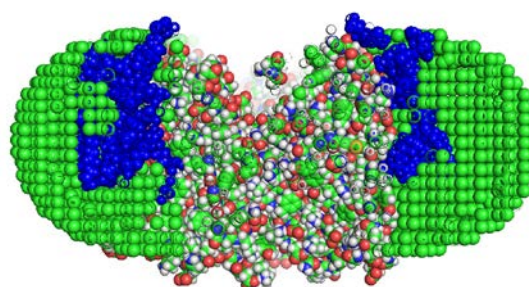
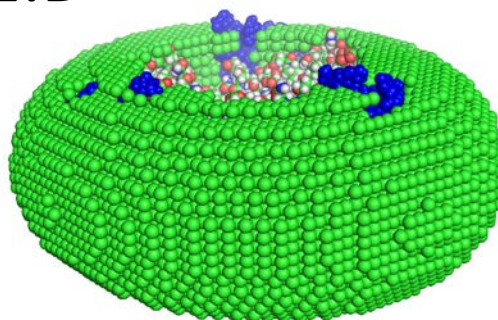
## S2:B

Sample	c, mg/ml	Scattering parameters*			Modelling detergent shell**						
		$I_0$	$R_g$	$D_{max}$	Protein (trans-membrane part) radius ( $\text{\AA}$ )	$R_g$ ( $\text{\AA}$ ) of the model	a, ( $\text{\AA}$ )	b, ( $\text{\AA}$ )	t, ( $\text{\AA}$ )	e	$\chi$
In vitro Refolded OmpF	0.42	441.63 $\pm 0.06$	46.2	128.9 $\pm 0.009$	35	45.9	35	40	5.0	1.13	1.53
In vitro Refolded OmpF-LPS complex	0.43	405.78 $\pm 0.06$	46.8	130.2 $\pm 0.008$	37	46.3	40	37	5.2	1.08	1.66
WT OmpF	0.65	439.67 $\pm 0.03$	47.6	129.8 $\pm 0.005$	37	47.6	40	39	5.3	1.08	1.97

S2:C



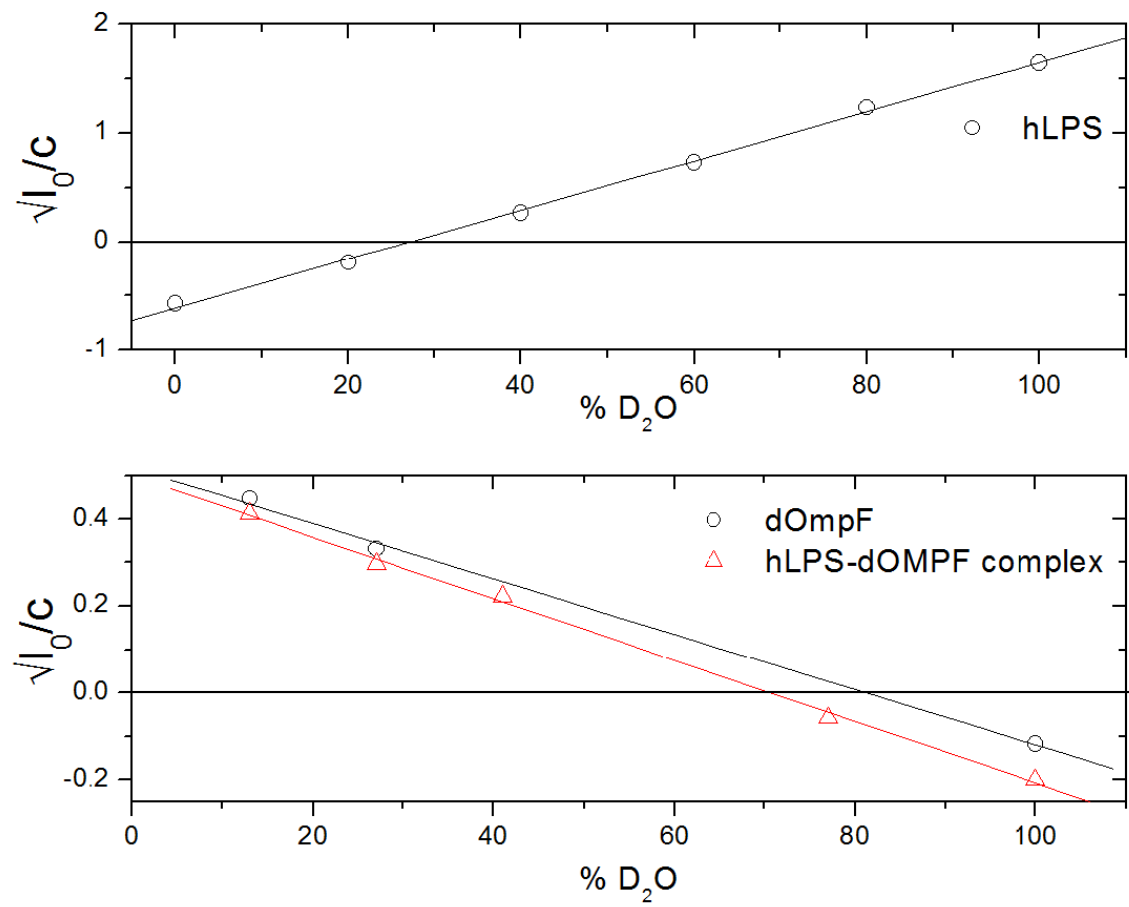
S2:D



**Figure S2** Small-angle X-ray scattering (SAXS). SAXS data for detergent solubilized OmpF-LPS complexes were collected on the beamline BM29 (1) at ESRF, France. (A) Scattering curves were recorded at a wavelength of 1.008 Å at a sample-detector distance of 2.85 m covering the momentum transfer range  $0.05 < q < 0.45 \text{ \AA}^{-1}$ , where  $q = (4\pi\sin\theta)/\lambda$  and  $2\theta$  is the scattering angle. The sample was gel-filtered prior to the SAXS experiment, the concentration of samples was 0.4 and 1 mg/ml, the experimental temperature was 20°C. Initial data processing and averaging were carried out according to (2). The scattering curves were converted to the real space pair-distribution function  $P(r)$  using Bayesian approach ([www. http://www.bayesapp.org/](http://www.bayesapp.org/)) (3, 4). OmpF-WT = samples purified from the bacterial outer membrane with naturally associated LPS; f-OmpF = *in vitro* refolded OmpF (LPS-free); F-OmpF-LPS complex = *in vitro* refolded OmpF mixed with Ra-LPS. The detergent shell of solubilized *in vitro* folded OmpF and OmpF-LPS complexes was modelled using program MEMPROT (5) using data for DDM micelles from (6). (B) The hydrophobic hydrocarbon tails of the detergent that assemble around the protein surface are modelled using Memprot (5) as an elliptical hollow torus of height  $a$  and cross-sectional minor and major axes  $b/e$  and  $b \times e$ , where  $e$  is the

ellipticity of the torus. The hydrophilic region occupied by the detergent polar headgroups is modelled as an exterior shell of constant thickness  $t$  surrounding the inner hydrophobic torus (5). \* SAXS data were obtained after a gel-filtration step for OmpF solubilised in 0.2 %DDM. \*\*Detergent shell modelling used a 2LPS per OmpF monomer model. (C) Fitted model for *in vitro* folded OMPF in DDM (Magenta) using Memprot. (D) Fitted model for WT OMPF purified with bound LPS in DDM using Memprot. Two LPS molecules (BLUE) per trimer. Note how the detergent micelle thickness (green) is extended compared to the LPS free sample in (C).

A)

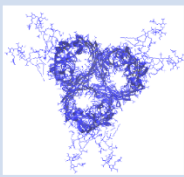
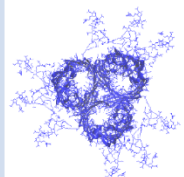
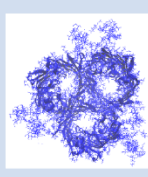
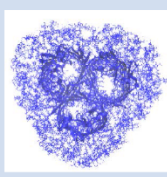




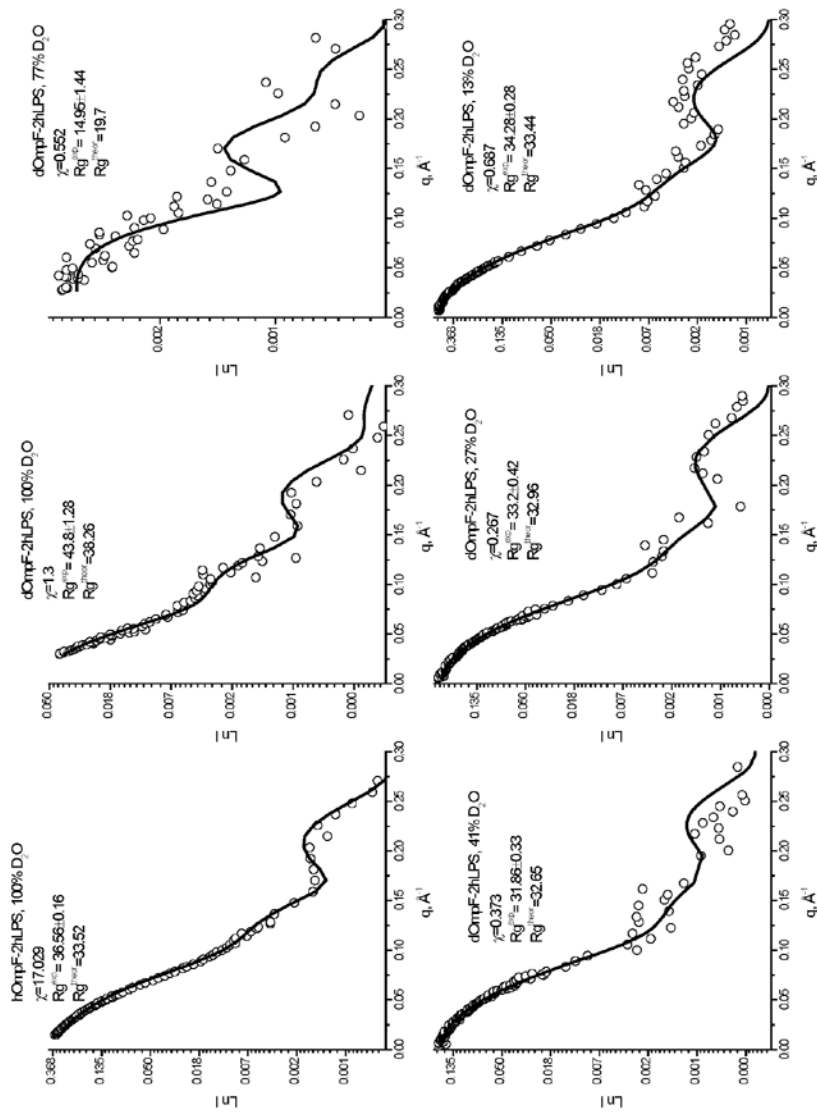
(B)

LPS/OmpF <sub>monomer</sub>	%D <sub>2</sub> O matchpoint
1:1	75.2
2:1	70.5
3:1	66.7
8:1	54.5
9:1	52.9

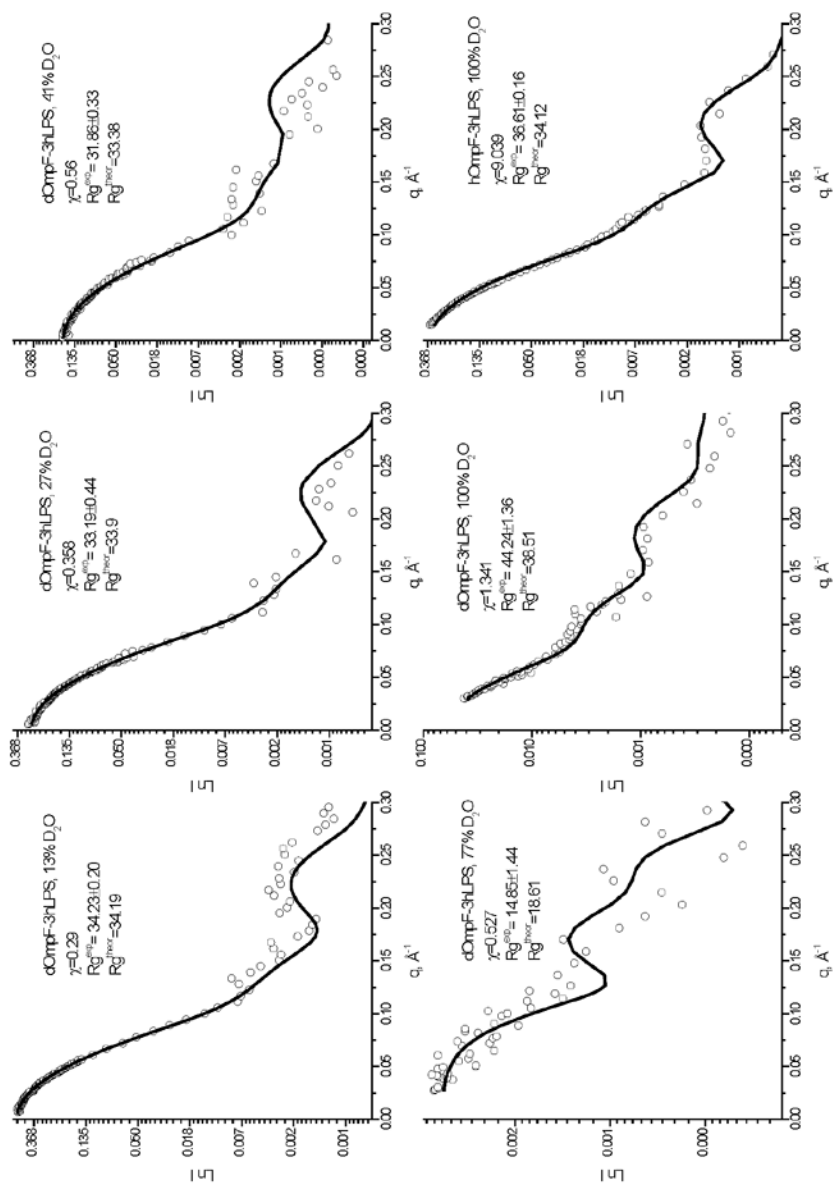
(C)

Contrast/Model	2LPS per monomer (extended)	3LPS per monomer (extended)	2LPS per monomer (compact)	8LPS per monomer
				
13% D <sub>2</sub> O (D/H)	0.687	0.29	0.878	3.478
27% D <sub>2</sub> O (D/H)	0.267	0.358	0.532	2.264
41% D <sub>2</sub> O (D/H)	0.373	0.56	0.726	2.042
77% D <sub>2</sub> O (D/H)	0.552	0.527	0.687	0.658
100% D <sub>2</sub> O (D/H)	1.3	1.341	1.731	1.043

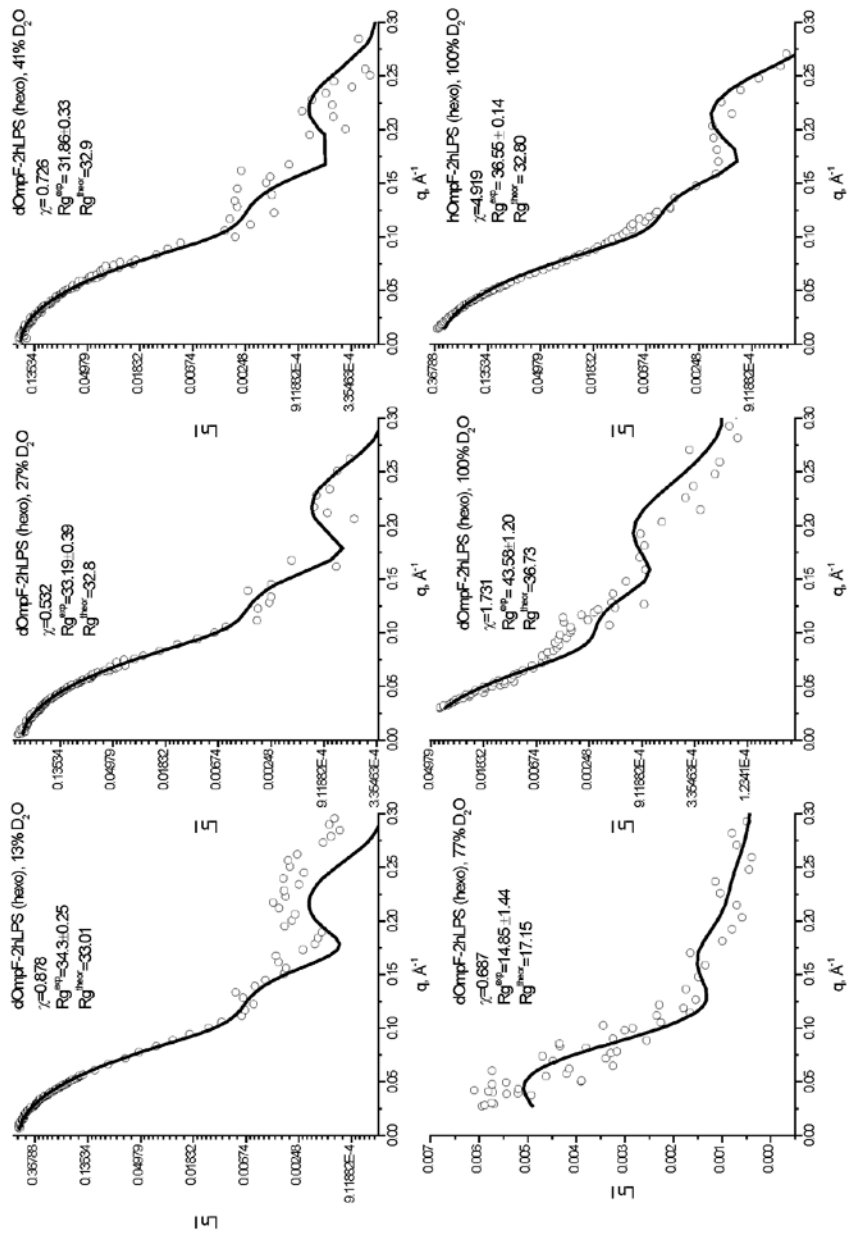
(D) 2LPS extended model



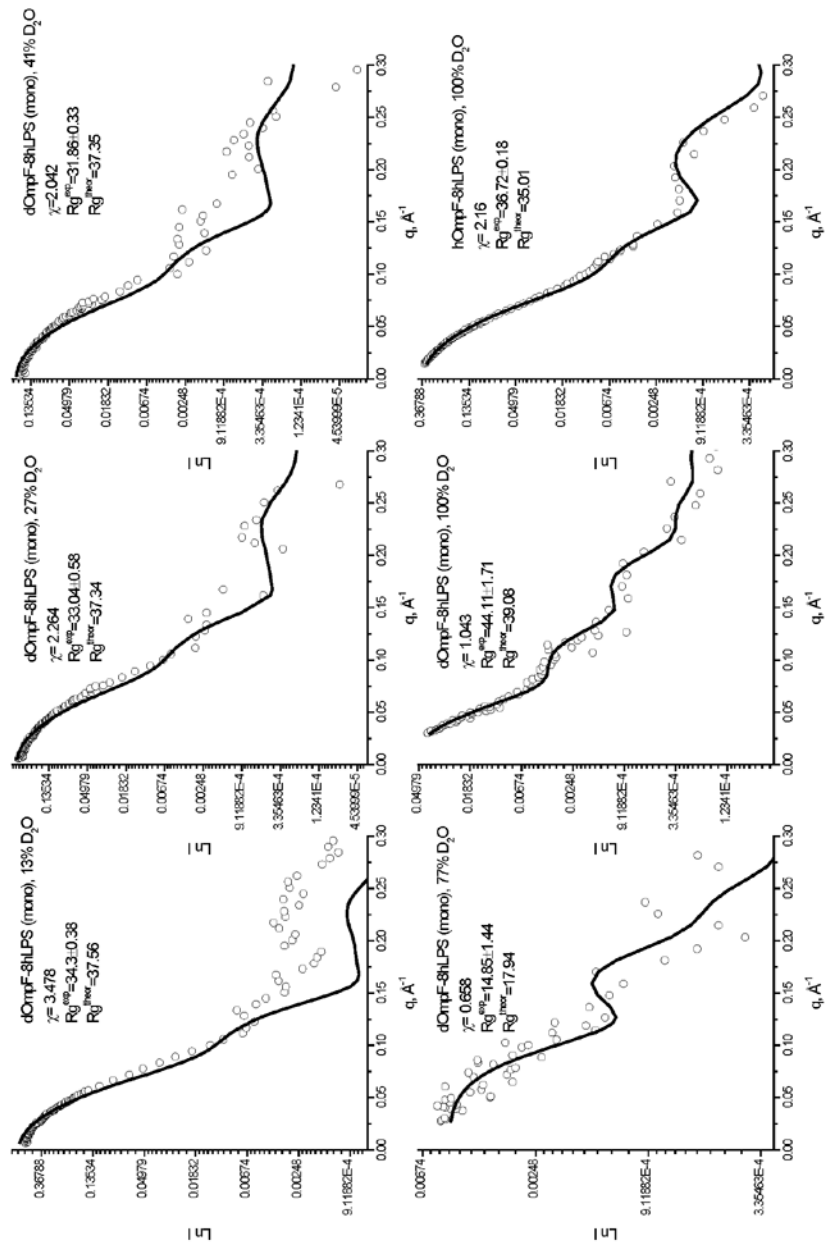
# (D) 3LPS extended model



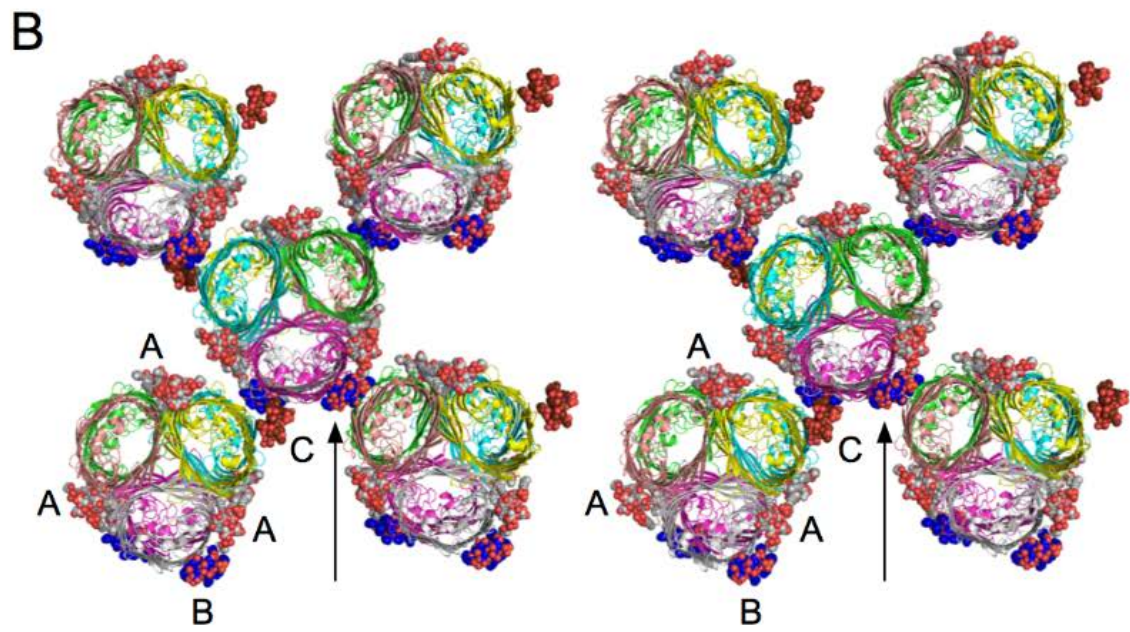
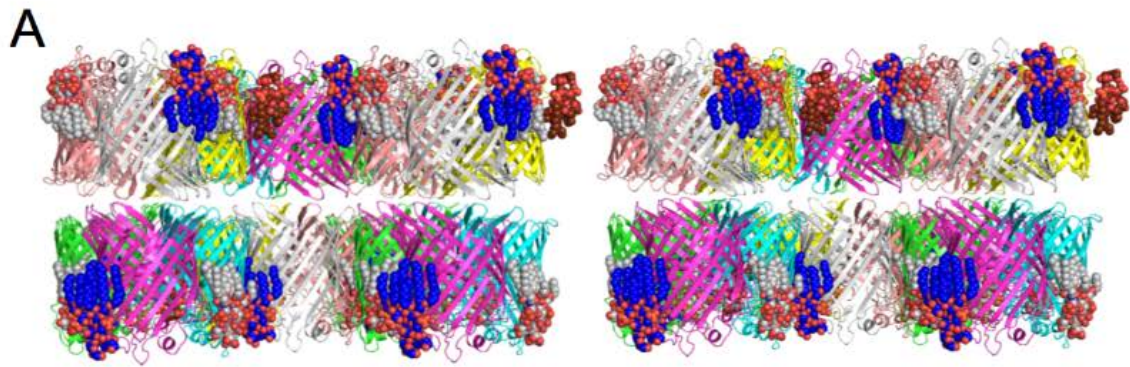
# (D) 2LPS compact model



# (D) 8LPS compact model

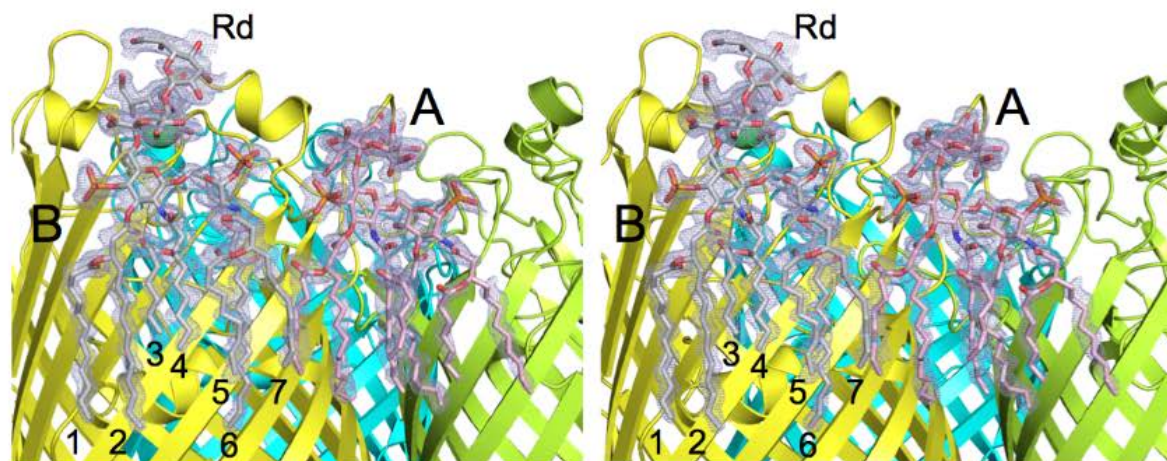


**Figure S3.** SANS Data. (A) Plots of  $\sqrt{I_0}$ /concentration versus % D<sub>2</sub>O to obtain point of zero intensity = match point for the samples shown. (B) Theoretical calculations for the match point of complexes with different levels of LPS made using the SASSIE contrast calculator. (<https://sassie-web.chem.utk.edu/sassie2/>) (7). (C) Quality of the CRYSON fit ( $\chi^2$ ) comparison for the four models. The data fitting by CRYSON suggests an extended than compact model for the complex. The results are not conclusive regarding whether there 2 or 3 molecules per OmpF monomer; fits are very poor for a complete annulus of 8 LPS per OMP monomer (8). (D) Scattering data modelled by CRYSON for each of the models in (C) (solid lines) compared with experimental scattering data for different neutron contrast data.

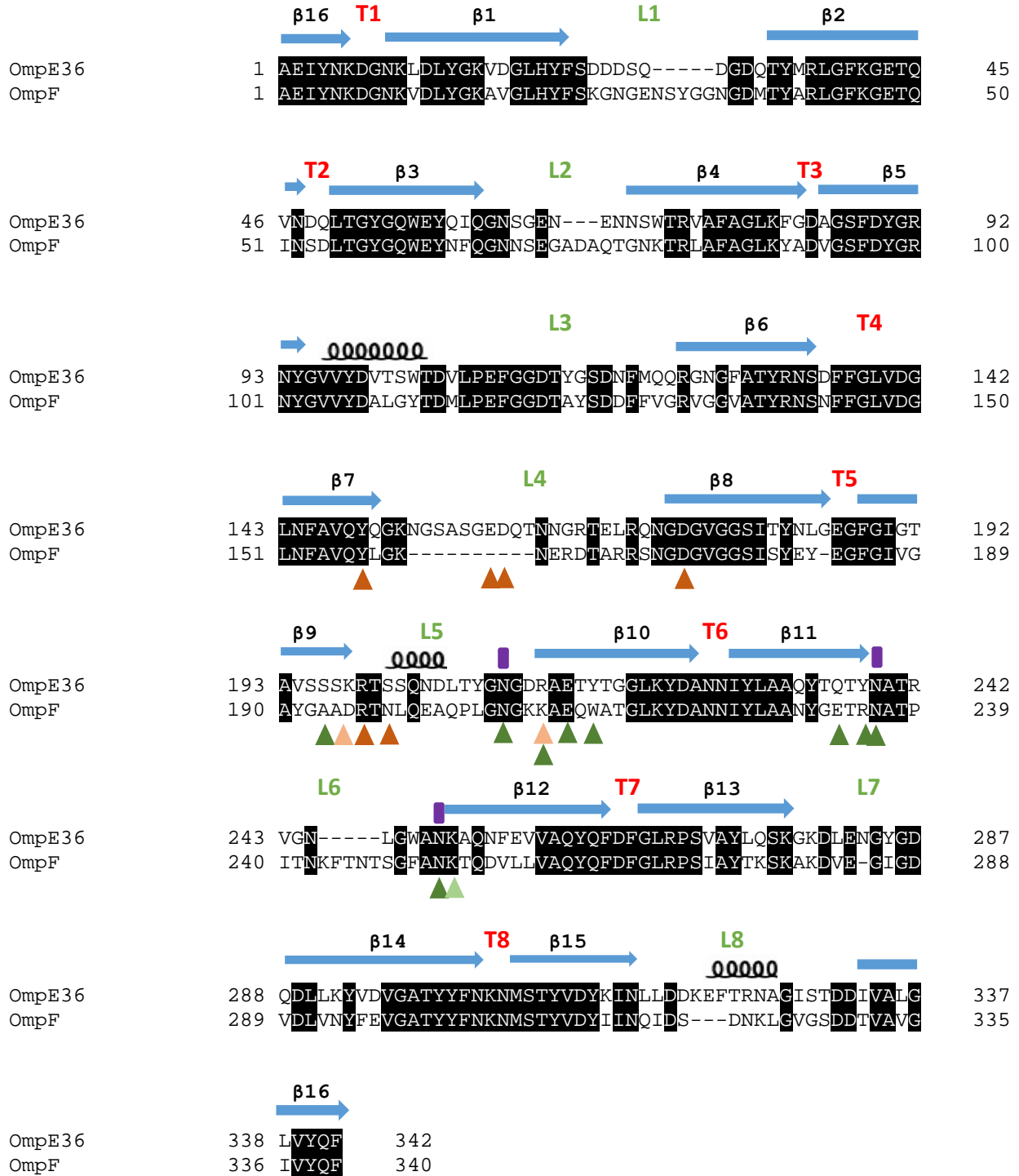


**Figure S4** Crystal packing of the OmpE36-LPS structure. Stereoviews from the side (A) and from the top (B), showing the arrangement of LPS molecules in the crystal. In B, the three different LPS sites are indicated (A, B, C), and the arrow highlights the important LPS B site which is sandwiched between two symmetry-related OmpE36 trimers.








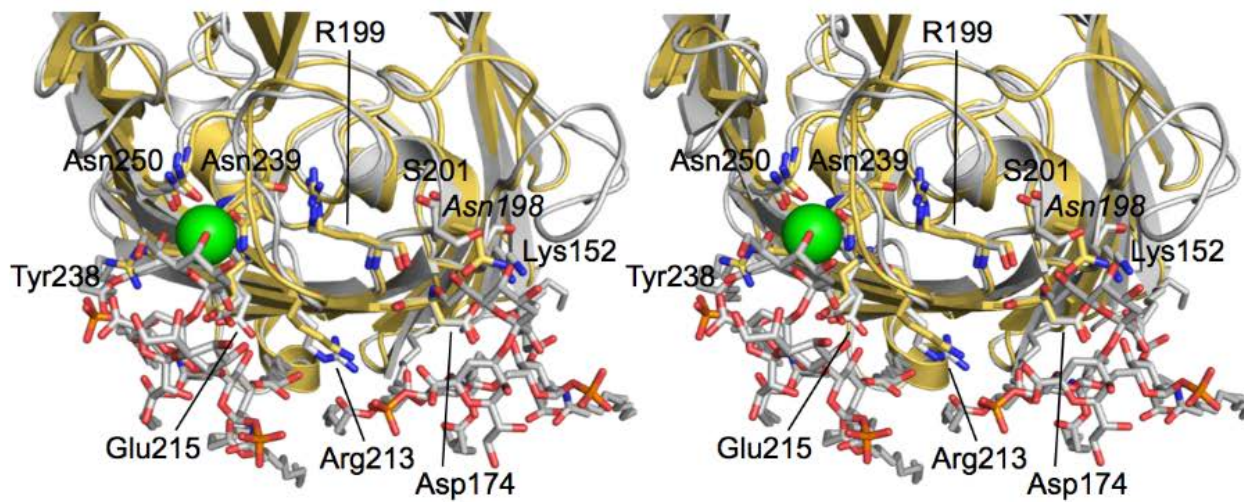


**Figure S5** LPS bound to OmpE36 is hepta-acylated. Stereo view from the side, showing 2Fo-Fc electron density (contoured at 1.0  $\sigma$ ) for LPS A and B. The seven lipid A acyl chains for LPS B have been numbered. The heptose subunit of Rd LPS B is labeled as well. The cartoon models for OmpE36 are colored differently from Fig. 5 to improve contrast with the electron density mesh.

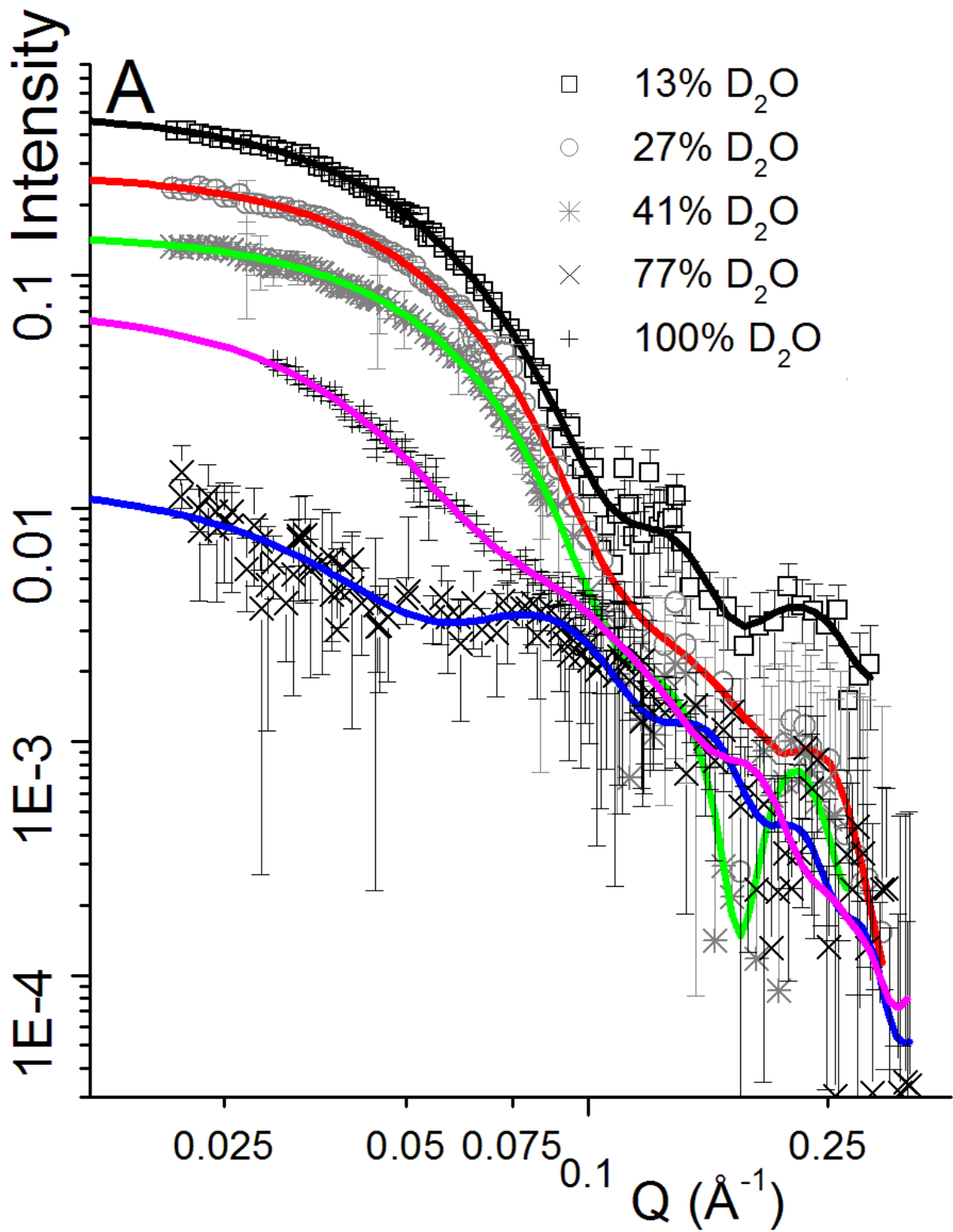


**Figure S6** Comparison of *E. coli* OmpF and OmpE36 from *Enterobacter cloacae*. (A) Sequence alignment of using Clustalw. Conserved residues are highlighted in black. The secondary elements of OmpE36 are indicated as follows: arrows,  $\beta$ -strands; coils,  $\alpha$ -helices; L1-L8, extracellular loops; T1-T8, periplasmic turns. The interactions of LPS moieties (LPS A and LPS B) with one of the monomers of OmpE36 have been shown by labelling the protein residues in following manner:

-  Residue (OmpE36):LPS A interaction; salt bridge (light orange triangle)
-  Residue (OmpE36):LPS A interaction; H-bond (dark orange triangle)
-  Residue (OmpE36):LPS B interaction; salt bridge (light green triangle)
-  Residue (OmpE36):LPS B interaction; H-bond (dark green triangle)
-  Residue (OmpE36):Calcium metal ion ionic interaction (purple bar)



**Figure S7.** The LPS binding sites of OmpE36 and *E. coli* OmpF are similar. Stereo view superposition of OmpE36 (grey) and *E. coli* OmpF (beige), using the program Coot (9), viewed from the extracellular side. Polar residues interacting with LPS A and B are labelled (only for OmpE36 for the sake of clarity). Calcium is indicated by a green sphere. The majority of residues interacting with OmpE36/OmpF are conserved (see also Figure S7).



**Figure S8.** Enlarged version of Figure 4A. In order to show data points more clearly, the same figure presented in the text is reproduced here. The figure legend in the main

text reads “Figure 4. SANS data indicates that LPS binds at the periphery of OmpF in SDS solution. (A) Scattering data for deuterated (d-)OmpF in complex with hydrogenous Ra-LPS after size exclusion chromatography. Fitted lines were generated by the program BayesApp to calculate the P(r) plots (see Table 1 for fitting parameters and supplementary data for an enlarged Fig. 4A).”

## Supplementary References

1. Pernot P, *et al.* (2010) New beamline dedicated to solution scattering from biological macromolecules at the ESRF. *Xiv International Conference on Small-Angle Scattering*, Journal of Physics Conference Series, ed Ungar G), Vol 247.
2. Franke D, Kikhney A, & Svergun D (2012) Automated acquisition and analysis of small angle X-ray scattering data. *Nucl. Instr. Meth. Phys. Res. A* 689:7.
3. Hansen S (2008) Simultaneous estimation of the form factor and structure factor for globular particles in small-angle scattering. *Journal of Applied Crystallography* 41(2):436-445.
4. Hansen S (2012) BayesApp: a web site for indirect transformation of small-angle scattering data. *Journal of Applied Crystallography* 45(3):566-567.
5. Perez J & Koutsioubas A (2015) Memprot: a program to model the detergent corona around a membrane protein based on SEC-SAXS data. *Acta Crystallogr D Biol Crystallogr* 71(Pt 1):86-93.
6. Berthaud A, Manzi J, Perez J, & Mangenot S (2012) Modeling Detergent Organization around Aquaporin-0 Using Small-Angle X-ray Scattering. *J. Am. Chem. Soc.* 134(24):10080-10088.
7. Curtis JE, Raghunandan S, Nanda H, & Krueger S (2012) SASSIE: A program to study intrinsically disordered biological molecules and macromolecular ensembles using experimental scattering restraints. *Comput. Phys. Commun.* 183(2):382-389.
8. Svergun DI, *et al.* (1998) Protein hydration in solution: Experimental observation by x-ray and neutron scattering. *Proceedings of the National Academy of Sciences of the United States of America* 95(5):2267-2272.
9. Emsley P & Cowtan K (2004) Coot: model-building tools for molecular graphics. *Acta Crystallographica Section D-Biological Crystallography* 60:2126-2132.